



Crystal Structures and Enzymatic Properties of a Triamine/Agmatine Aminopropyltransferase from *Thermus thermophilus*

Mio Ohnuma^{1*}†, Tadashi Ganbe²†, Yusuke Terui¹, Masaru Niitsu³, Takao Sato², Nobuo Tanaka², Masatada Tamakoshi¹, Keijiro Samejima³, Takashi Kumasaka^{2,4} and Tairo Oshima^{1,5}

¹Department of Molecular Biology, Tokyo University of Pharmacy and Life Science, Tokyo 192-0392, Japan

²Department of Life Science, Tokyo Institute of Technology, Yokohama 226-8501, Japan

³Faculty of Pharmaceutical Science, Josai University, Saitama 530-0248, Japan

⁴Japan Synchrotron Radiation Research Institute, Hyogo 679-5198, Japan

⁵Institute of Environmental Microbiology, Kyowa Kako Co., Ltd., Tokyo 194-0035, Japan

Received 25 December 2010;

received in revised form

10 March 2011;

accepted 13 March 2011

Available online

31 March 2011

Edited by G. Schulz

Keywords:

agmatine;
aminopropyltransferase;
crystal structure;
polyamine;
Thermus thermophilus

To maintain functional conformations of DNA and RNA in high-temperature environments, an extremely thermophilic bacterium, *Thermus thermophilus*, employs a unique polyamine biosynthetic pathway and produces more than 16 types of polyamines. In the thermophile genome, only one spermidine synthase homolog (SpeE) was found and it was shown to be a key enzyme in the pathway. The catalytic assay of the purified enzyme revealed that it utilizes triamines (norspermidine and spermidine) and agmatine as acceptors in its aminopropyl transfer reaction; therefore, the enzyme was denoted as a triamine/agmatine aminopropyltransferase (TAAPT). We determined the crystal structures of the enzyme complexed with and without the aminopropyl group donor *S*-adenosylmethionine. Despite sequence and structural similarity with spermidine synthases from other organisms, a novel C-terminal β -sheet and differences in the catalytic site were observed. The C-terminal module interacts with the gatekeeping loop and fixes the open conformation of the loop to recognize larger polyamine substrates such as agmatine and spermidine. Additional computational docking studies suggest that the structural differences of the catalytic site also contribute to recognition of the aminopropyl/aminobutyl or guanidium moiety of the substrates of TAAPT. These results explain in part the extraordinarily diverse polyamine spectrum found in *T. thermophilus*.

© 2011 Elsevier Ltd. All rights reserved.

*Corresponding author. 3-34-1 Nishiikebukuro, Toshima-ku, Tokyo 171-8501, Japan. E-mail address: mioohnuma@rikkyo.ac.jp.

† M.O. and T.G. contributed equally to this work.

Present address: M. Ohnuma, Research Information Center for Extremophile, Rikkyo University, Tokyo 171–8501, Japan.

Abbreviations used: ACAPT, agmatine/cadaverine aminopropyl transferase; AdoDATO, *S*-adenosyl-1,8-diamino-3-thiooctane; dcSAM, decarboxylated *S*-adenosylmethionine; EDTA, ethylenediaminetetraacetic acid; SPDS, spermidine synthase; SPMS, spermine synthase; 3D, three-dimensional; TAAPT, triamine/agmatine aminopropyltransferase; TmSPDS, *Thermotoga maritima* SPDS; TtTAAPT, *T. thermophilus* TAAPT.

Introduction

Polyamines are basic molecules containing more than two amino nitrogen atoms and are involved in cell proliferation through interactions with negatively charged biomolecules such as DNA, RNA, membrane lipids, and ATP.¹ They are ubiquitously distributed in prokaryotes and eukaryotes. The most common polyamines in eukaryotes are putrescine, spermidine, and spermine. Polyamine composition varies between species: flowering plants and most animal cells contain all three polyamines, while many prokaryotes lack spermine. However, extreme thermophiles often produce unusual polyamines; for instance, *Thermus thermophilus* contains more than 16 polyamines including long polyamines such as caldopentamine [1,15-diamino-4,8,12-triazapentadecane, $\text{NH}_2(\text{CH}_2)_3\text{NH}(\text{CH}_2)_3\text{NH}(\text{CH}_2)_3\text{NH}(\text{CH}_2)_3\text{NH}_2$] and caldohexamine [1,19-diamino-4,8,12,16-tetraazanonadecane, $\text{NH}_2(\text{CH}_2)_3\text{NH}(\text{CH}_2)_3\text{NH}(\text{CH}_2)_3\text{NH}(\text{CH}_2)_3\text{NH}_2$],² and branched polyamines such as mitsubishine [tris(3-aminopropyl)amine, $[\text{NH}_2(\text{CH}_2)_3]_3\text{N}$] and tetrakis(3-aminopropyl)ammonium ($[\text{NH}_2(\text{CH}_2)_3]_4\text{N}^+$).³ Cellular concentrations of these unusual polyamines increase with elevation of growth temperature, suggesting roles in biochemical reactions at high temperature.⁴ The unusual long and branched

polyamines effectively stabilize double- and single-stranded nucleic acids, respectively.⁵

In the general biosynthetic pathway of polyamines, putrescine can be formed directly from ornithine by the action of ornithine decarboxylase. Plants and most bacteria possess an additional or alternative pathway to form putrescine from arginine;^{1,6,7} arginine is decarboxylated to form agmatine by arginine decarboxylase, and agmatine is subsequently converted to putrescine directly by agmatine ureohydrolase or sequentially by agmatine deiminase and *N*-carbamoylputrescine amidohydrolase. Spermidine and spermine are synthesized from putrescine and spermidine, respectively, via spermidine synthase (SPDS) and spermine synthase (SPMS) by the addition of an aminopropyl group from decarboxylated *S*-adenosylmethionine (dcSAM, dcAdoMet), leaving 5'-methylthioadenosine (MTA) (Fig. 1).⁸

In our previous work, we proposed that *T. thermophilus* employs a novel biosynthetic pathway; that is, arginine is converted to agmatine followed by aminopropylation to form *N*¹-aminopropylagmatine. *N*¹-Aminopropylagmatine is then hydrolyzed to produce spermidine by the SpeB (agmatine ureohydrolase) homolog.⁹ In this new pathway, agmatine is aminopropylated by SpeE to form *N*¹-aminopropylagmatine. SpeE is the only SPDS

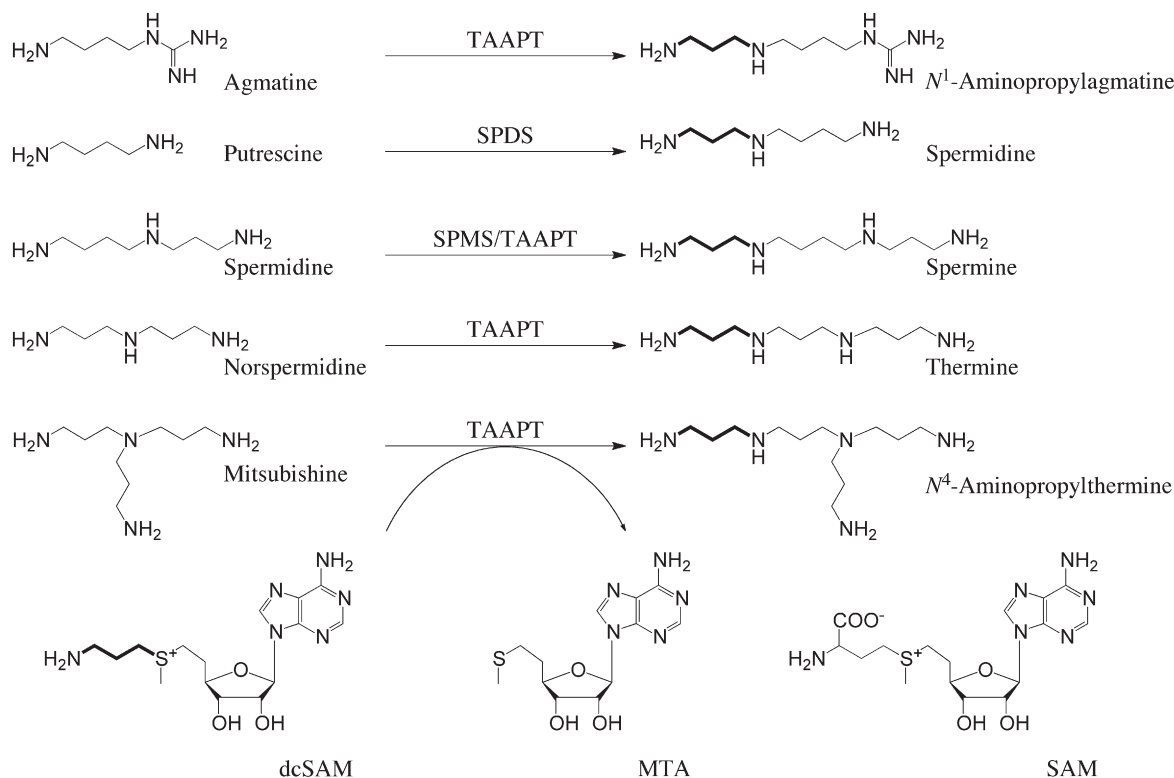


Fig. 1. Structural formula of polyamines and the reaction of aminopropyl transfer by aminopropyltransferases. The aminopropyl moiety of dcSAM (shown in bold lines) is transferred to the amino terminus of substrates, and polyamine products are obtained.

homologue found in the genome of *T. thermophilus* HB8. The amino acid sequence of SpeE exhibits similarity to that of SPDS, but is more similar to that of thermospermine synthase,¹⁰ and enzymatic characterization revealed that the enzyme does not accept putrescine as a substrate but does accept agmatine and triamines [norspermidine (1,7-diamino-4-azaheptane) and spermidine] as described below (Fig. 1). Therefore, the SPDS homologue, which is pivotal for the formation of spermidine and formerly named agmatine/spermidine aminopropyltransferase, is now renamed as a triamine/agmatine aminopropyltransferase (TAAPT).

Our current research has determined the three-dimensional (3D) structure and enzymatic properties of *T. thermophilus* TAAPT (TtTAAPT) in order to clarify the molecular basis of its unique substrate specificity. In some bacteria, archaea, and eukaryotes, spermidine is generally synthesized from putrescine by the addition of an aminopropyl group from dcSAM. However, TtTAAPT does not act on putrescine, but on agmatine or triamines. Therefore, it is important to know the molecular mechanism by which the thermophile enzyme rejects putrescine as a substrate even though agmatine and spermidine contain a putrescine moiety in their structures.

Results and Discussion

Subunit structure

The molecular mass of TtTAAPT was estimated with a calibrated Superdex 200 HR 10/30 column. The enzyme was eluted from this column as a single symmetrical peak corresponding to 130 kDa (data not shown). Since the calculated molecular mass of the TtTAAPT monomer is 36 kDa, we concluded that TtTAAPT forms a homotetramer in solution. The subunit structures of human SPDS, SPMS,^{11–13} *Plasmodium falciparum* SPDS,¹⁴ and *Escherichia coli* SPDS^{15,16} are dimers. On the other hand, *Thermotoga maritima* SPDS (hereinafter TmSPDS)¹⁷ is a tetramer. Generally, thermophilic enzymes have a higher oligomerization state than their mesophilic homologues, leading to an enlarged buried surface area and increased packing density.^{18–21} TtTAAPT would appear to employ the same strategy to increase thermostability.

Substrate specificity

TtTAAPT converts agmatine to *N*¹-aminopropylagmatine as previously reported.⁹ Despite the fact that many unique polyamines are produced by the thermophile, only one *speE* orthologue was found in the *T. thermophilus* genome. Therefore, the enzyme

was thought to be capable of accepting not only agmatine but also various other polyamines as substrates by analogy with the putrescine aminopropyltransferase of the leguminous plant alfalfa, which accepts not only putrescine but also spermidine and spermine as a substrate.²² As shown in Fig. 2a, in addition to agmatine, norspermidine and spermidine were efficiently aminopropylated by the enzyme. When homospermidine [1,9-diamino-5-azanonane, $\text{NH}_2(\text{CH}_2)_4\text{NH}(\text{CH}_2)_4\text{NH}_2$], mitsubishine, or thermine [1,11-diamino-4,8-diazaundecane, $\text{NH}_2(\text{CH}_2)_3\text{NH}(\text{CH}_2)_3\text{NH}(\text{CH}_2)_3\text{NH}_2$] was used as a substrate, the enzyme showed low activity. Only faint activities (<10% of spermidine) were detected for diaminopropane [$\text{NH}_2(\text{CH}_2)_3\text{NH}_2$], putrescine, spermine, and caldopentamine under the assay conditions employed. Therefore, the enzyme was named as a triamine/agmatine aminopropyltransferase (TAAPT). TtTAAPT effectively accepted linear polyamines whose lengths are 8–12 Å. Although the length of mitsubishine was calculated to be 10 Å, the effect of steric hindrance by the branched polyamine would decrease aminopropyltransferase activity. TmSPDS also accepts various polyamines as substrates, such as putrescine, diaminopropane, and spermidine.¹⁷ Putrescine is the best substrate for TmSPDS. The difference in substrate preference might result from the size of the binding cavity, gatekeeping loop, and C-terminal extra β -sheet as described below.

As shown in Table 1, we measured kinetic parameters for dcSAM and polyamines whose lengths are 8–12 Å. The affinity of TtTAAPT for dcSAM was similar to that of *E. coli* SPDS¹⁵ ($K_m=2.2 \mu\text{M}$), human SPDS²³ (0.9 μM), and TmSPDS²³ (0.75 μM) and higher than that of *Pyrococcus furiosus* agmatine/cadaverine aminopropyl transferase (ACAPT)²⁴ (20 μM). The affinity of TtTAAPT for spermidine (1.73 μM) and norspermidine (0.57 μM) was 11- to 38-fold higher than that of *E. coli* SPDS¹⁵ (12 μM), human SPDS²³ (19 μM), and TmSPDS²³ (20 μM). Similarly, the affinity of TtTAAPT for agmatine (0.77 μM) was 10-fold higher than that of *P. furiosus* ACAPT²⁴ for agmatine (7.6 μM). Norspermidine is the best polyamine as a substrate with the highest catalytic efficiency. Spermidine was calculated to have the highest k_{cat} value among the polyamines. The k_{cat} value of TtTAAPT (0.37 s^{-1}) for agmatine was fourfold higher than that of *P. furiosus* ACAPT²⁴ (0.1 s^{-1}). The catalytic efficiency (k_{cat}/K_m) for norspermidine is only about twofold higher than that for agmatine and spermidine. Therefore, these three polyamines would be used as substrates *in vivo*. Based on the activity of TtTAAPT, *T. thermophilus* produces aminopropylagmatine, spermine, and thermine from agmatine, spermidine, and norspermidine, respectively. Aminopropylagmatine is a precursor of spermidine.⁹ Spermine and thermine were the

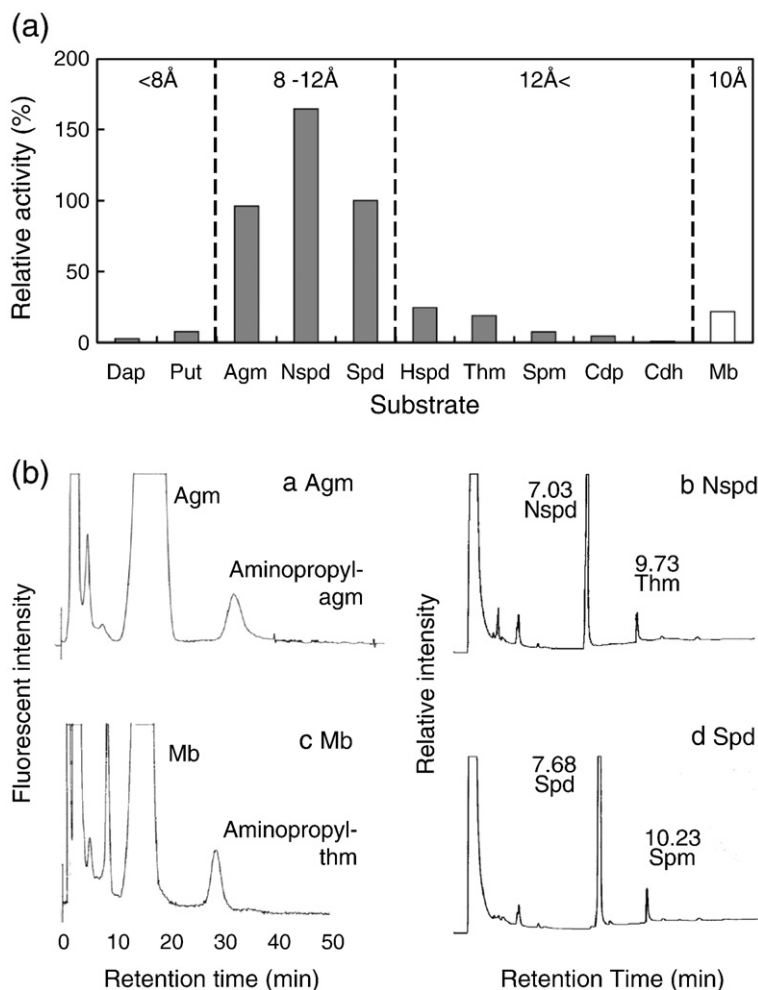


Fig. 2. (a) Substrate preference of TtTAAPT. Activities are represented as percentage of activity of the reaction using spermidine. Agmatine (Agm) and linear polyamines (Dap, diaminopropane; Put, putrescine; Nspd, norspermidine; Spd, spermidine; Hspd, *sym*-homospermidine; Thm, thermine; Spm, spermine; Cdp, caldopentamine; Cdh, caldoxamine), gray bars; branched polyamine (Mb, mitsubishine), white bar. The average of duplicate reactions is shown. The reaction was performed at pH 9 at 37 °C for 30 min with 10 ng of TtTAAPT used in each reaction. Calculated length of agmatine and polyamines is shown in the graph area. Minimized energy of polyamines was calculated using ChemDraw3D. Length of polyamines was calculated using ViewerLite. (b) Identification of reaction products by HPLC or gas chromatography. Products of *in vitro* reactions using (a) agmatine and (c) mitsubishine as substrates were analyzed by HPLC. Products formed by *in vitro* reaction using (b) norspermidine and (d) spermidine were analyzed by gas chromatography. The 900- μ l reaction mixtures consisted of 0.1 M Tris-Cl buffer (pH 9), 5 mM dithiothreitol, 0.36 mM unlabeled dcSAM, and polyamines (1 mM norspermidine, 2 mM spermidine or agmatine, or 4 mM mitsubishine) as the substrate. Reaction mixtures were incubated with the purified enzyme (4.5 μ g for norspermidine, 9 μ g for spermidine, agmatine, and mitsubishine) at 37 °C for 180 min. Aminopropylagm, N^1 -aminopropylagmatine; Aminopropylthm, N^4 -aminopropylthermine.

major compounds when the cells were cultured at 60 and 80 °C, respectively.²⁵ When mitsubishine was used as a substrate, the k_{cat} value was similar to that when agmatine was used as a substrate; however, catalytic efficiency (k_{cat}/K_m) was very low due to very poor affinity of the enzyme for mitsubishine. This is understandable for a branched polyamine, which might be affected by steric

hindrance. Moreover, the fact that the reaction product for mitsubishine [see below, Fig. 2b(c)] was not found in *T. thermophilus* cells²⁵ suggests that mitsubishine would be unlikely to be used as a substrate *in vivo* and that the aminopropylation reaction of mitsubishine has no physiological importance.

Identification of reaction products

Identification of reaction products

TtTAAPT reaction products were determined by HPLC and gas chromatography (Fig. 2b). Our previous study suggested that the thermophile SpeE converts agmatine to N^1 -aminopropylagmatine [Fig. 2b(a)].⁹ As shown in Fig. 2b(b), the thermophile enzyme converted norspermidine to thermine. When spermidine is aminopropylated, spermine and/or thermospermine [1,12-diamino-4,8-diazadodecane, $\text{NH}_2(\text{CH}_2)_3\text{NH}(\text{CH}_2)_3\text{NH}$

Table 1. K_m and k_{cat} of TtTAAPT at 37 °C, pH 9.0

	K_m (μM)	k_{cat} (s^{-1})	k_{cat}/K_m ($\text{M}^{-1} \text{s}^{-1}$)
Spermidine	1.73	0.65	3.8×10^5
Norspermidine	0.57	0.53	9.2×10^5
Agmatine ^a	0.77	0.37	4.8×10^5
Mitsubishine	38.31	0.29	7.6×10^3
dcSAM	1.64	0.73	4.5×10^5

^a From Ohnuma *et al.*⁹

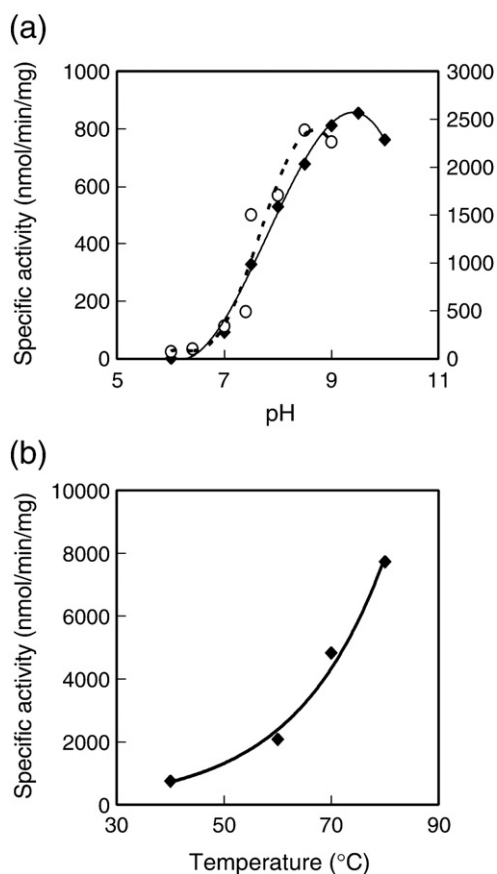


Fig. 3. pH and temperature dependence of the enzyme activity. 1 mM spermidine was used as a substrate and 10 ng of the enzyme was used in each reaction. (a) pH dependency. Buffers used were potassium phosphate (at pH 6–7.4), Tris-HCl (pH 7.5–9), and glycine-NaOH (pH 9.5 and 10). Reactions were performed at 37 °C for 30 min (filled diamonds, left *y*-axis) and 60 °C for 20 min (open circles, right *y*-axis). (b) Temperature dependency. The reaction was performed in Tris-HCl (pH 8) for 30 min at 37 °C, 20 min at 60 °C, 10 min at 70 °C, and 5 min at 80 °C.

$(\text{CH}_2)_4\text{NH}_2]$ can be formed depending on the reaction specificity of the enzyme. If the thermophile enzyme aminopropylates the aminopropyl group of spermidine, thermospermine can be synthesized. If the enzyme specifically recognizes the aminobutyl group of the spermidine, the product should be spermine. If the enzyme possesses loose specificity, then both thermospermine and spermine can be formed. Gas chromatography analyses revealed that the TtTAAPT specifically converts spermidine only to spermine [Fig. 2b(d)]. When mitsubishine is used as a substrate, tetrakis(3-aminopropyl)ammonium and/or N^4 -aminopropylthermine can be formed. Since heptafluorobutyrate tetrakis(3-aminopropyl)ammonium decomposes spontaneously to mitsubishine and heptafluorobutyrate monoamine,²⁶

HPLC analysis was used to identify the product [Fig. 2b(c)]. TtTAAPT converted mitsubishine to N^4 -aminopropylthermine, but not to tetrakis(3-aminopropyl)ammonium.

pH and thermal dependency

As shown in Fig. 3a, the effect of pH on enzyme activity was investigated over a pH range of 6–10 at 37 °C, and the enzyme showed highest aminopropyltransferase activity at around pH 9.5. When the reaction was performed at 60 °C, the optimum pH of the reaction was shifted to 8.5. Enzyme activity was barely affected by the presence or absence of 1 mM magnesium ion and 1 mM ethylenediaminetetraacetic acid (EDTA) at 60 °C, pH 8.5 (data not shown). The rate of the reaction was significantly increased by temperature elevation up to 80 °C (Fig. 3b).

To evaluate the pH and temperature stabilities of the enzyme, CD spectra were measured. The spectrum of the enzyme at pH 10.4 (Fig. 4a) was nearly identical to that at pH 7.0 (data not shown). This result suggests that the enzyme is stable at around pH 10 at room temperature. Figure 4b shows heat denaturation profiles at pH 10.4. The protein

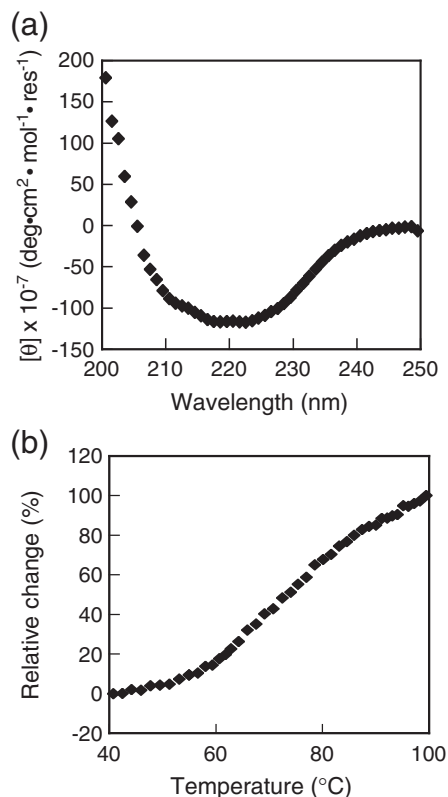


Fig. 4. pH and temperature stability of the enzyme. (a) Far-UV CD spectra of native enzyme. (b) Heat denaturation profile at 222 nm. The solution contained 0.2 mg/ml enzyme (1.4 μM as tetramer enzyme) in 20 mM $\text{Na}_2\text{B}_4\text{O}_7$ at pH 10.4.

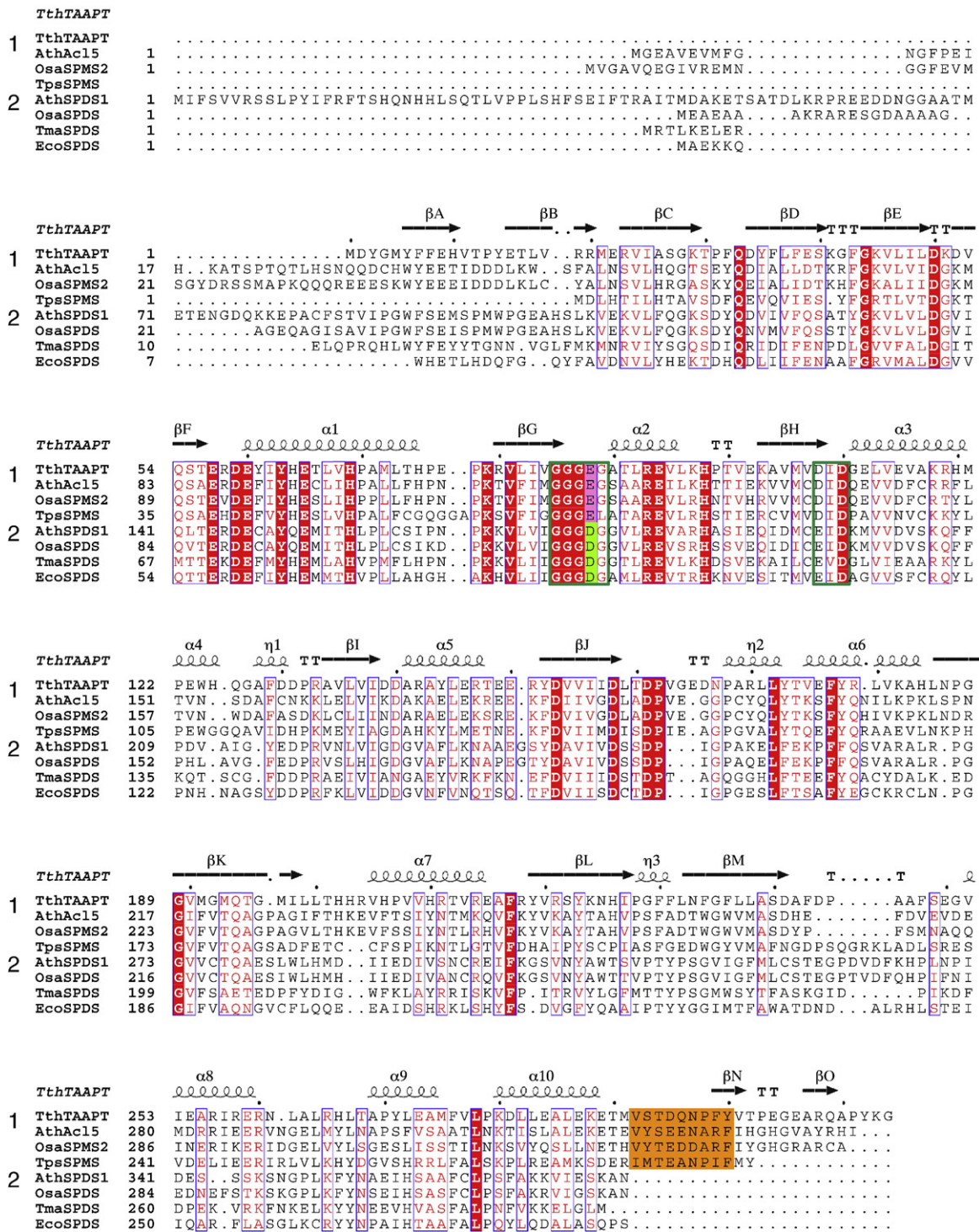


Fig. 5. Sequence alignment of characterized aminopropyltransferases. Group 1 (TAAPT/AtACL5): *TthTAAPT*: TAAPT from *T. thermophilus*; *AthACL5*: ACL5 from *A. thaliana*;²⁹ *OsaSPMS2*: SPMS from *O. sativa*; *TpsSPMS*: SPMS from *T. pseudonana*.¹⁰ Group 2 (SPDS): *AthSPDS*: SPDS from *A. thaliana*;^{30,31} *OsaSPDS*: SPDS from *O. sativa*;³² *TmaSPDS*: SPDS from *T. maritima*;¹⁷ *EcoSPDS*: SPDS from *E. coli*.³³ The first line shows the secondary structural elements of TtTAAPT. The GGG(D/E)G motif and (E/D)(I/V)D motif, which are important for binding of polyamine and dcSAM, are indicated by green boxes. Residues D and E of GGG(D/E)G motif, critical to preference of polyamine, are indicated by a lime and pink background, respectively. Residues assigned as homologous only in group 1 by the program ESPript are indicated by an orange background.

was only gradually denatured upon elevation of temperature and was not completely denatured at least until 100 °C at pH 7.0 (not shown). The enzyme proved to be a very high pH- and heat-stable protein, as shown in Fig. 4b.

The amino acid sequence of the *speE* gene homologue contains no cysteine residues. This is consistent with the fact that the enzymes of aerobic thermophiles tend to contain fewer cysteine residues, in particular, on the protein surface.²⁷ It has been reported that the C^β-S^γ bond of cysteine residues is labile at high temperature in aerobic conditions.²⁸

Overall structure

The amino acid sequence of TtTAAPT exhibited higher similarity with *Arabidopsis* ACL5, thermospermine synthase, than with SPDS (Fig. 5). The crystal structure of TtTAAPT contained the two independent subunits in an asymmetric unit. The TmSPDS structure [Protein Data Bank (PDB) ID 1INL]¹⁷ is superimposed on TtTAAPT with a root-mean-square deviation (RMSD) of 1.0 Å. The overall structure of TtTAAPT also resembles other SPDS structures. The RMSDs with other SPDS structures are 1.3 Å from *P. furiosus* (PDB ID 1MJF),²⁴ 1.5 Å from *Bacillus subtilis* (PDB ID 1IY9), 1.3 Å from *Arabidopsis thaliana* (PDB ID 1XJ5), and 1.4 Å from human (PDB ID 1ZDZ, replaced by 2O05).²³ Since the molecular mass of TtTAAPT was estimated to be 130 kDa by gel-filtration analysis as described, we conclude that the biological assembly was a homotetramer with a crystallographic 2-fold axis (Fig. 6a, PDB ID 1UIR). Each subunit was composed of two

domains: the N-terminal domain (residues 1–58) consisted of six β-strands (βA–βF), and the C-terminal domain (residues 59–314) consisted of 10 α-helices (α1–α10) and nine β-strands (βG–βO) (Figs. 5 and 6a).

The N-terminal βA and βB strands are the main components of the tetramer interface and form an eight-stranded antiparallel β-barrel by each chain. From the two strands, Tyr6, Phe8, and Val18 protrude into the inside of the barrel and make a hydrophobic core. Met1 and Tyr3 participate in the hydrophobic core, and the N-terminal tail region covers the barrel. The outside of the barrel is packed with a four-stranded antiparallel β-sheet composed of βC, βD, βE, and βF. This structure is similar to the TmSPDS tetramer interface;¹⁷ therefore, we infer that the oligomerization of thermophilic enzymes reduces the size of the molecular surface and contributes to the unusual thermostability of the enzyme.

The C-terminal domain possesses a Rossmann-like fold that is mainly composed of a seven stranded β-sheet (βG, βH, βI, βJ, βK, βL, and βM). This motif accepts the substrate dcSAM. Therefore, the C-terminal domain contained the catalytic site, even though the catalytic cleft lay between both domains. The cleft is large enough to accept the additional polyamine substrate. For the lid of the catalytic cleft, there is a loop structure between βJ and α6, called the gatekeeping loop, which is flexible in the apoenzyme of TmSPDS.¹⁷ Two β-strands closest to the C-terminus, βN and βO, are found only in TtTAAPT and interact with the gatekeeping loop (Fig. 6b, PDB ID 3ANX). Including this region, no significant difference between apoenzyme and binary complex can be observed in their 3D structures.

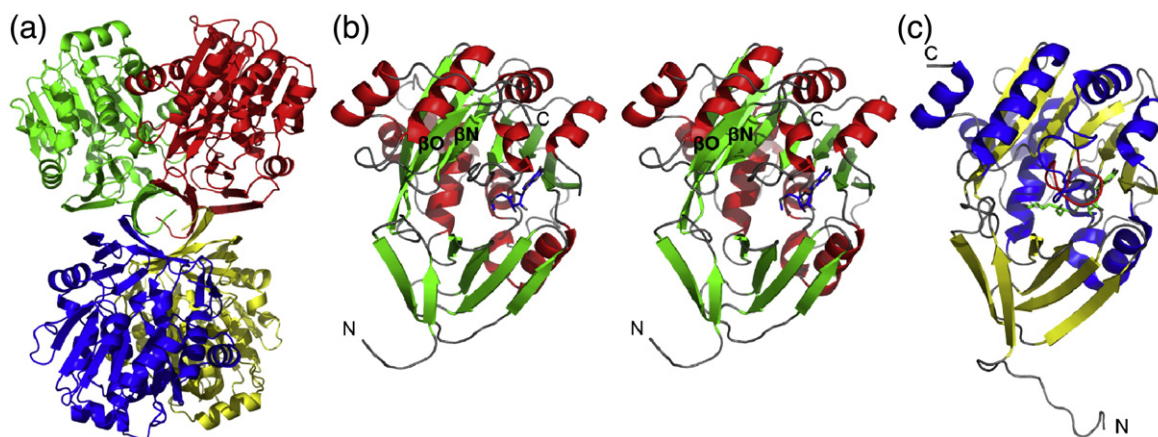


Fig. 6. Structure of TtTAAPT. (a) Ribbon diagram of TtTAAPT tetramer. Each subunit is colored differently. (b) Stereo view of the TtTAAPT monomer in ribbon diagram representation. The adenosyl part of SAM is shown by blue sticks. The two β-strands (βN, βO) of the C-terminal module are also shown. (c) Ribbon diagram of TmSPDS monomer represented in the same orientation as in (b). Alternative conformation of the gatekeeping loop is colored in red. Multisubstrate inhibitor AdoDATO is shown by green sticks.

Structure of the dcSAM binding site

We attempted to obtain TtTAAPT complexed with SAM, dcSAM, polyamines, or inhibitors, but we only succeeded in binding SAM with TtTAAPT. In TtTAAPT complexed with SAM, the electron density of SAM was observed only for its adenosyl moiety (Fig. 7a). The methionyl moiety of SAM showed ambiguous electron densities. SAM has a carboxylate group that is absent in dcSAM; therefore, its negative charge might affect binding to the catalytic cleft. The methionyl moiety might be extended flexibly to the polyamine binding site, and/or it could be digested by the hydrolytic reaction producing MTA and homoserine. The following discussion is based on the models constructed using the TmSPDS-S-adenosyl-1,8-diamino-3-thiooctane (AdoDATO) complex structure.

Binding of the adenine moiety is mostly similar to the binding mode of AdoDATO to TmSPDS; the adenine ring is sandwiched between Ile109 (corresponding to Val122 in TmSPDS) and Leu159 (corresponding to Ser171 in TmSPDS) by the stacking interactions with these hydrophobic residues. A hydrogen bond is formed between the N⁶ amino group of SAM and Asp140. Although Val122 of TmSPDS behaves in the same way as Ile109 of TtTAAPT, Ser171 of TmSPDS does not contribute to the interaction with the adenine ring in the way that Leu159 of TtTAAPT does because of its polarity. Instead, Leu182 of TmSPDS contributes to the interaction with the adenine ring. On the other hand, the equivalent residue of the TmSPDS Leu182 in TtTAAPT is Leu172, which cannot make the hydrophobic interaction with the adenine. A hydrogen bond between the N⁶ atom of adenine and Asp140 in TtTAAPT is also observed in TmSPDS, and it consists of the side chain of Asn152 (corresponding to Asp140 of TtTAAPT). Recognition of the ribose moiety is performed by the interaction between the side chain of Asp108 and the hydroxyl groups of the ribose in positions 2' and 3', similar to the TmSPDS structure.

From the structural and sequential alignment with TmSPDS, Tyr63 and Asp158 in TtTAAPT also have the same orientation as the corresponding residues of TmSPDS (Tyr76 and Asp170, respectively), which are thought to be catalytic residues, and TtTAAPT Glu88 and His64 might interact with the aminopropyl group of dcSAM. The motif for the dcSAM binding scaffold is conserved in all members of the SPDS/SPMS family consisting of the sequence (L/I/V)GGG(D/E)G(G/A). The fifth residue of the motif is variable, and there is a difference between TtTAAPT and TmSPDS (Fig. 5). In the case of TtTAAPT, the side chain of that residue, Glu88, is bulkier than that of Asp101, the corresponding residue in TmSPDS; therefore, it could not insert the aminopropyl moiety of dcSAM into the deeper hole of TtTAAPT. As a result, this might affect the position of dcSAM, especially its S^γ atom, a key atom of the aminopropyl transfer reaction.

Structure of polyamine binding site

The interaction between polyamine and enzyme is thought to be weak because of the failure of the co-crystallization with norspermine, spermine, and agmatine. This is consistent with the report that the putrescine moiety of AdoDATO is not enveloped completely in the structure of TmSPDS. It suggests that the aminopropyl enzyme was not formed and the aminopropyl transfer reaction is a single-displacement mechanism,³⁴ not a sequential ping-pong mechanism.

The polyamine binding site shows larger structural differences with that of TmSPDS than the dcSAM site. In particular, Asp161 of TtTAAPT makes an interaction with the Gln194 side chain and shows a positional difference of approximately 2 Å in C^α atoms from the corresponding residue Asp173 of TmSPDS, which might play a role in anchoring a terminal amino group of putrescine in TmSPDS. From the superimposition of AdoDATO onto TtTAAPT, the carboxyl group of Asp161 may

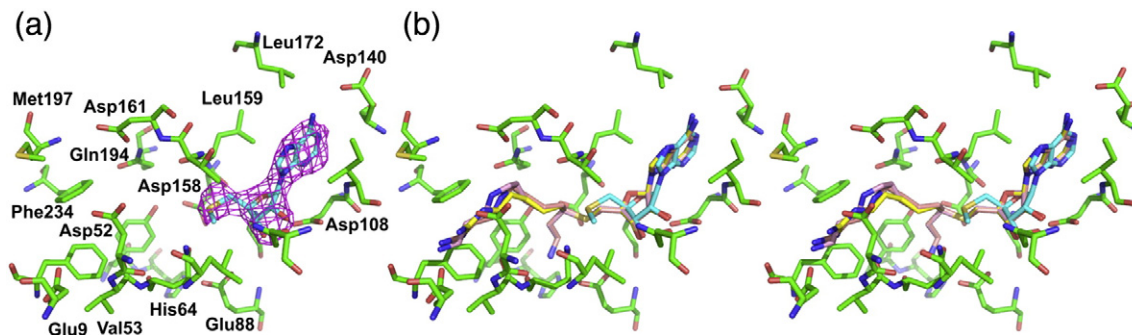


Fig. 7. Substrate binding of TtTAAPT. (a) The complex structure around the substrate binding site. The protein portion of TtTAAPT and the adenosyl part of SAM are shown in green and cyan, respectively. The omit $F_o - F_c$ map contoured with 3σ is also shown in magenta. (b) The docking models superimposed to the binary complex structure. The models containing agmatine and spermidine moieties are shown in yellow and pink, respectively.

interact with the guanidium group of agmatine in a bidentate manner. However, Asp161 and Phe234 are relatively close to each other in the observed structures, and there is not enough space for the bulky guanidium group between the two residues. It is also suggested by the fact that the two residues repelled the guanidium group in the energy-minimized binding model (data not shown). To make the interaction, the side chain of Asp161 should break its interaction with Gln194 and move to an open space, the polyamine binding pocket, as with TmSPDS. In the case of spermidine, its tail amino group might be too close to interact with Asp161 because of its length, and it might interfere with Met197.

Another conformational difference in the vicinity of the active site is found in the region from Phe230 to Leu232. TtTAAPT can accept substrates longer than putrescine because this region is shorter by one residue and forms a wider space than that of TmSPDS. This is similar to *E. coli* SPDS, which has a larger binding cavity.¹⁶ There is another similarity to *E. coli* SPDS. Steric hindrance may be a contributing factor to the preference of polyamine substrate. Human SPDS has high specificity for putrescine as an amine acceptor, while TmSPDS can act on spermidine even though activity on putrescine is much higher than that on spermidine.²³ In human SPDS, a wall of the binding pocket formed by Trp28 and Pro242 side chains prevents the binding of an additional aminopropyl group of longer substrates. On the other hand, these residues are replaced by Tyr23 and Pro240 in TmSPDS and provide more space to accommodate larger substrates. The binding pocket of TtTAAPT is even wider, because Glu9 is the closest residue to the polyamine, while Trp28 and Tyr23 are closest in human SPDS and TmSPDS, respectively,²³ and the rigid proline, which interferes with the guanidium group of agmatine or the aminopropyl group of spermidine in human SPDS and TmSPDS, is replaced by Phe234 (Fig. 1).

To investigate other possible substrate-recognition mechanisms, computational ligand docking was performed (Fig. 7b). The results suggested that the middle portion of the polyamine substrates was accommodated by the movement of Asp161, and the end portion was positioned toward the other side of the active-site wall against Asp161. There are two conserved acidic amino acids, Glu9 and Asp59. The extended guanidium or N-terminal group interacts with the former glutamate residue, which is conserved in both SPDSs and SPMSs. Additionally, the carbonyl oxygen of Val53 located at the same wall may interact with the secondary amine group of spermidine. TtTAAPT also recognizes norspermidine, which is shorter than spermidine by one methylene group. However, the positional shift of Asp161 might also be caused by the amino acid insertion in the β_j - η_2 loop. This insertion is not conserved with other SPMSs; therefore, Asp161

might not contribute to recognition, and the adaptation to agmatine recognition might be unique to TtTAAPT. In the docking study, it is still not clear how the central amine group in spermidine and norspermidine is recognized. In the case of spermidine, its molecular structure is not symmetric; therefore, its substrate recognition is important to the selectivity of the product as described before. Hence, the candidates for substrate recognition should be examined by site-directed mutagenesis in future studies.

Structure of gatekeeping loop and C-terminal extra β -sheet

A large structural difference between TtTAAPT and SPDSs is also found at the loop region β_j - α_6 formed by residues 159–172. This region was described as the gatekeeping loop in the TmSPDS structure and is important for recognition of dcSAM and putrescine. In the case of TtTAAPT, the main-chain atoms of Pro162 O and Gly164 N of this loop formed hydrogen bonds with the main-chain atoms of Val301 in the novel C-terminal β -sheet, and there is also a hydrophobic interaction among Pro162 and Val163, Tyr173, Phe299, Val301. Accordingly, the loop structure is fixed open, and is not changed upon the SAM binding. In contrast, this loop in TmSPDS becomes ordered from a disordered conformation upon binding with AdoDATO in the active site. As described below, several structural analyses revealed that this structural change is widely shared in SPDSs.

The structural rearrangement from SPDS to TAAPT is achieved as follows: the position of the carboxyl group of Asp161 of TtTAAPT is occupied by Glu206 in the closed conformation of TmSPDS. Gly196 of TtTAAPT, equivalent to the glutamate, provides the room for the Asp161 side chain. Here, Trp214 occupies the open structure of TmSPDS. Since Asp173 of TmSPDS has to enter the space to make an interaction with putrescine, the χ_1 angle of Trp214 rotates and opens the space.

The structural change of the gatekeeping loop is also essential to capture short molecules such as putrescine in SPDSs. To interact with the substrate, the gatekeeping loop has to be close to putrescine. The closed conformation narrows the catalytic cavity and encloses the bound dcSAM. On the other hand, TtTAAPT fixes the loop structure by the interaction with the extra C-terminal β -sheet, and the fixed conformation is enough to allow interactions with longer polyamines. Therefore, the gatekeeper mechanism differs between TtTAAPT and SPDSs. Recently, structures of human, nematode, and apicomplexan SPDSs were determined.^{14,23,35} The human structure shows a structure similar to the closed loop of the TmSPDS–AdoDATO complex.

Nematode SPDS structure was determined in ligand-free form, and its gatekeeping loop is disordered even with the presence of proline residues. The gatekeeping loop of the apicomplexan SPDS is partially disordered and stabilization of the loop was observed in the dcSAM complex. Hence, this flexibility of the loop seems to be common in SPDSs.

The flexibility of the loop may be related to substrate specificities. Although the substrate specificity of TmSPDS changes with reaction temperature,²³ this was not the case with TtTAAP. Furthermore, TtTAAPT does not recognize putrescine and the apparent order of its activity is norspermidine > spermidine ≥ agmatine at either 60 or 37 °C (data not shown), suggesting that the

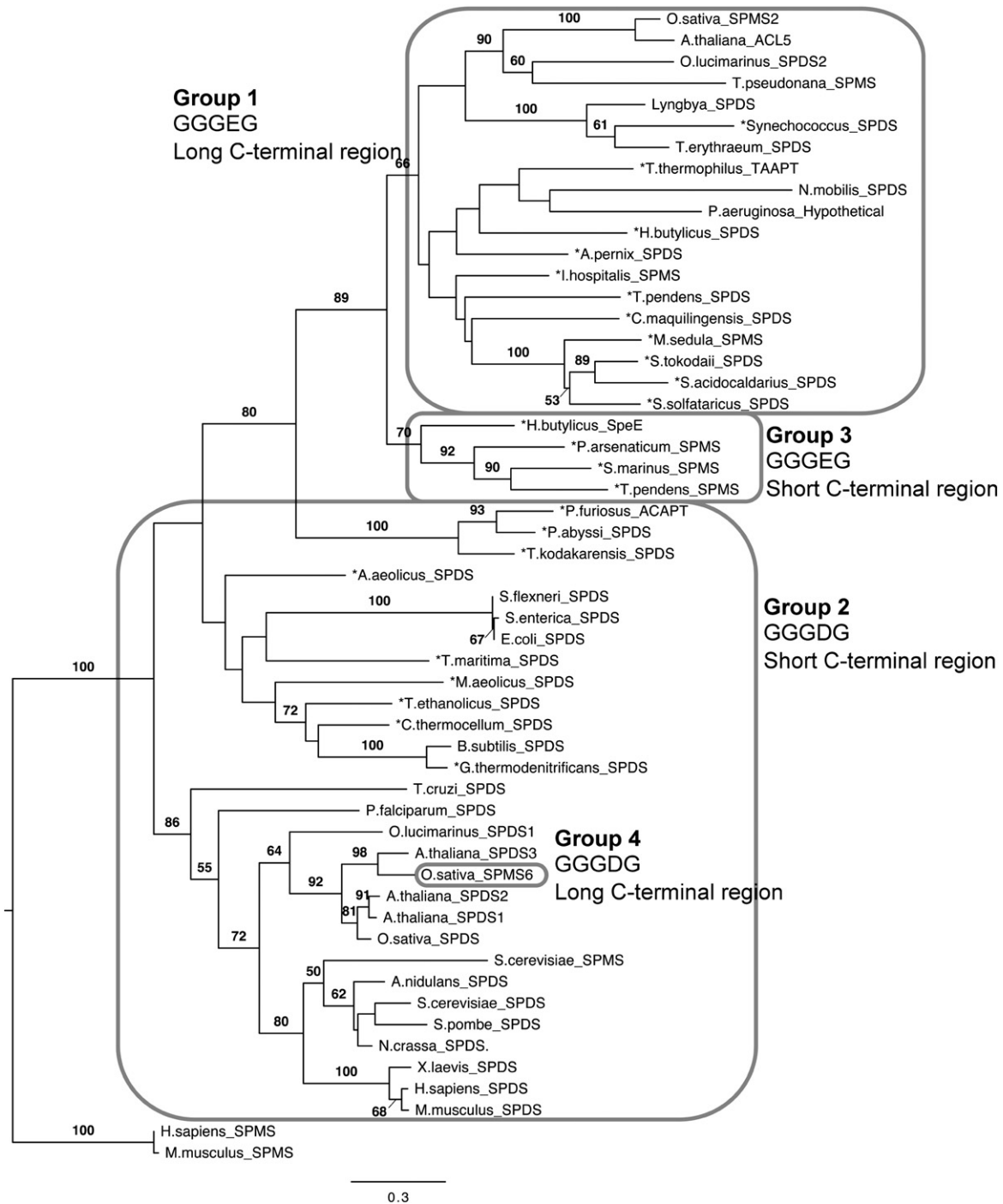


Fig. 8 (legend on next page)

gatekeeping loop is fixed independent of temperature change.

Biosynthesis of polyamines in *T. thermophilus*

The substrate specificity of TtTAAPT does not fully explain the biosynthesis of the unique polyamines such as homospermine [1,13-diamino-4,9-diazatridecane, $\text{NH}_2(\text{CH}_2)_3\text{NH}(\text{CH}_2)_4\text{NH}(\text{CH}_2)_4\text{NH}_2$], thermospermine, pentaamines, and tetrakis(3-aminopropyl)ammonium, of which thermospermine is a major component.²⁵ TtTAAPT accepted spermidine as a substrate, but the product was only spermine and no thermospermine was formed [Fig. 2b(b)]. TtTAAPT might provide some portion of homospermine in the cell, since TtTAAPT had low activity for homospermidine (Fig. 2a). The thermophile enzyme did not produce thermospermine *in vitro* [Fig. 2b(d)]. For the production of thermospermine, at least two reactions are possible: (1) another aminopropyltransferase might be present in the cell to aminopropylate the aminopropyl group of spermidine; (2) an aminobutylation capability might be present in the cell to produce thermospermine by reactions analogous to the production of homospermidine from putrescine in some mesophilic bacteria.³⁶ Norspermidine (Caldine) has been detected in thermophile cells in a relatively large amount,²⁵ and this triamine cannot be produced by TtTAAPT. Moreover, when spermidine was added

to minimal medium, the *speBE* double disruptant could produce tetrakis(3-aminopropyl)ammonium (M.O., unpublished data). Production of tetrakis(3-aminopropyl)ammonium requires another aminopropyltransferase in the cell. Nevertheless, only one aminopropyltransferase homologue (*speE*) is present in the *T. thermophilus* genome. These unique polyamines could be produced by other enzymes that exhibit low homology to known aminopropyltransferases, or the enzymes may belong to a different family. Elucidation of the biosynthesis of the long and branched polyamines is the subject of our future studies.

Phylogenetic relationship of TtTAAPT

As shown in Fig. 5, polyamine aminopropyltransferase was classified into two groups. These correspond to the ACL5 group (GGGEG motif) and the SPDS/SPMS group (GGGDG motif), which Knott and coworkers detected by comparison of various SPDSs and SPMSs.¹⁰ *A. thaliana* ACL5²⁹ and the SPMS homolog of *Thalassiosira pseudonana*, which produces thermospermine instead of spermidine or spermine,¹⁰ also has a long C-terminal region, similar to TtTAAPT. To examine the phylogenetic relationship of TtTAAPT, we performed maximum likelihood analyses with 54 polyamine aminopropyltransferases. Based on the phylogenetic tree shown in Fig. 8, polyamine aminopropyltransferases can be classified into four groups

Fig. 8. Phylogenetic relationship of the polyamine aminopropyltransferase proteins. The polyamine aminopropyltransferase proteins, which exhibit sequence similarity to TtTAAPT, were found by using PSI-BLAST. Proteins that were experimentally uncharacterized were included in these sequences. A multiple alignment obtained using ClustalW was checked and manually edited. The phylogenetic tree was constructed by maximum likelihood methods using the RAXML Web server³⁷ and FigTree software (<http://www.tree.bio.ed.ac.uk/software/figtree>). Bootstrap support values obtained from 100 pseudo-replicates of the data set were indicated only when the value was higher than 50. Branch lengths were drawn proportional to the amount of difference based on genetic distance; the scale bar indicates the number of substitutions per site. Human and mouse SPMS were used as an outgroup. These proteins are classified into four groups according to the GGG(D/E)G motif and the C-terminal region (group 1 proteins have a GGGEG motif and a long C-terminal region; group 2 proteins have a GGGDG motif and a short C-terminal region; group 3 proteins have a GGGEG motif and a short C-terminal region; group 4 proteins have a GGGDG motif and a long C-terminal region). This classification is described in detail in the [Results and Discussion](#) section. The asterisk represents thermophiles or hyperthermophiles. Hypothetical, hypothetical protein. *Aeropyrum pernix* K1 (NP_147478), *Aquifex aeolicus* VF5 (NP_213033), *A. thaliana* (NP_001078605, NP_173794, NP_177188, NP_001078749), *Aspergillus nidulans* FGSC A4 (XP_658291), *B. subtilis* subsp. *subtilis* str. 168 (NP_391630), *Caldivirga maquilensis* IC-167 (ZP_01710548), *Clostridium thermocellum* ATCC 27405 (YP_001037122), *E. coli* K12 (NP_414663), *Geobacillus thermodenitrificans* NG80-2 (YP_001127432), *Homo sapiens* (NP_003123, NP_004586), *Hyperthermus butylicus* DSM 5456 (YP_001012598, YP_001012280), *Ignicoccus hospitalis* KIN4/I (YP_001435222), *Lyngbya* sp. PCC 8106 (ZP_01619477), *Metallosphaera sedula* DSM 5348 (YP_001192315), *Methanococcus aeolicus* Nankai-3 (YP_001324799), *Mus musculus* (NP_033298, NP_033240), *Neurospora crassa* OR74A (XP_960907), *Nitrococcus mobilis* Nb-231 (ZP_01128528), *O. sativa* (NP_001046395, NP_001057773, NP_001059438), *Ostreococcus lucimarinus* CCE9901 (XP_001420452, XP_001418368), *P. falciparum* 3D7 (XP_001347972), *Pseudomonas aeruginosa* PAO1 (NP_253462), *Pyrobaculum arsenaticum* DSM 13514 (YP_001152549), *Pyrococcus abyssi* GE5 (NP_125890), *P. furiosus* DSM 3638 (NP_577856), *Saccharomyces cerevisiae* (NP_015394, NP_013247), *Salmonella enterica* subsp. *enterica* serovar Typhi str. CT18 (NP_454779), *Schizosaccharomyces pombe* 972h- (NP_596015), *Shigella flexneri* 2a str. 301 (NP_706074), *Staphylothermus marinus* F1 (YP_001041435), *Sulfolobus acidocaldarius* DSM 639 (YP_255324), *Sulfolobus solfataricus* P2 (NP_342261), *Sulfolobus tokodaii* str. 7 (NP_376216), *Synechococcus* sp. JA-2-3B'a(2-13) (YP_476322), *T. pseudonana* CCMP1335 (XP_002294468), *Thermoanaerobacter ethanolicus* CCSD1 (ZP_05492908), *Thermococcus kodakarensis* KOD1 (YP_182560), *Thermofilum pendens* Hrk 5 (YP_919533, YP_920782), *T. maritima* MSB8 (AAD35738), *T. thermophilus* HB8 (1UIR_A), *Trichodesmium erythraeum* IMS101 (YP_720760), *Trypanosoma cruzi* strain CL Brener (XP_811725), *Xenopus laevis* (NP_001084875).

according to the GGG(D/E)G motif, the binding site for AdoDATO in TmSPDS,¹⁷ and the C-terminal region. Group 1 proteins have a GGGE motif and a long C-terminal region, such as TtTAAT, *A. thaliana* ACL5,²⁹ and *T. pseudonana* SPMS.¹⁰ Group 2 proteins have a GGGDG motif and a short C-terminal region. Many conventional SPDSs and SPMSs found in bacteria, plants, and animals can be classified into group 2. Group 3 proteins have a GGGE motif and a short C-terminal region. Only polyamine aminopropyltransferases from Crenarchaeota were classified into group 3. Group 4 protein has a GGGDG motif and a long C-terminal region. *Oryza sativa*_SPMS6 is the single protein that was classified into group 4 among 54 analyzed proteins. The amino acid sequence of its long C-terminal region was not conserved with that of group 1. The function of the long C-terminal region of Group 4 is unknown.

Groups 1 and 3 (GGGE motif containing) proteins are clearly separated from groups 2 and 4 (GGGDG motif containing) proteins. In group 2 proteins, bacterial and eukaryotic proteins are clearly separated. In the eukaryotic clades, plants, animals, and fungi formed individual clades. Groups 1 and 3 separated into distinct clades. In group 1 proteins, plant, cyanobacterial, and Chromalveolata enzymes, which contain plastid, were grouped within a clade.

In addition, there is a conserved MTA binding site at Glu220 and Ile221 of human SPMS.¹² The corresponding amino acids of most aminopropyltransferases in group 2 are Glu and Ile, respectively, with some exceptions (e.g., TmSPDS Glu121 and Val122, *B. subtilis* SPDS Asp107 and Ile108). We found that all aminopropyltransferases in groups 1 and 3, which have the GGGE motif, have an Asp-Ile sequence (e.g., TtTAAPT Asp108 and Ile109, *A. thaliana* ACL5 Asp130 and Ile131; Fig. 5). Sequences of both human SPMS and *P. furiosus* agmatine/cadaverine aminopropyltransferase are GGGDG and EID, even though they accept spermidine and agmatine as a substrate, respectively.^{12,24} TtTAAPT recognizes substrates differently from human SPMS and *P. furiosus* agmatine/cadaverine aminopropyltransferase. The GGG(D/E)G and (E/D)(I/V)D motif is important for binding of polyamine and dcSAM,^{12,17} and our results demonstrate that the long C-terminal region is important for recognition of longer polyamines as substrates. Therefore, other proteins classified as group 1 polyamine aminopropyltransferase could have altered substrate-recognition mechanism and have important roles in producing uncommon polyamines, which are often found in thermophiles and plants.

Conclusion: Molecular basis of substrate specificity of TtTAAPT

The structure of TtTAAPT reveals a novel C-terminal module composed of two β -strands. This

module interacts with the gatekeeping loop and fixes the loop structure. Since TtTAAPT is similar to the SPMS family in accepting longer substrates and also the C-terminal extension in the primary structure, this module might be shared with long polyamine synthases in the thermophile. The binary complex structure with SAM reveals a recognition scheme similar to that of TmSPDS for the methylthioadenosine portion, while the predicted recognition scheme of the putrescine moieties of the longer polyamines, such as agmatine and spermidine, reveals that the moieties were located and recognized along the opposite wall of the active-site cleft. The structure of TtTAAPT is the first crystal structure of a group 1 polyamine aminopropyltransferase.

Materials and Methods

Protein expression and purification

The SpeE (TtTAAPT) protein was overexpressed in *E. coli* BL21 (DE3) cells carrying pESE8⁹ by induction with 0.5 mM isopropyl β -D-thiogalactopyranoside (IPTG) at 37 °C. Cells were grown in Luria-Bertani medium for 3 h after IPTG induction and were harvested by centrifugation at 4200g for 15 min at 4 °C. The cell pellet was suspended in 20 mM Tris-HCl, 50 mM NaCl, and 1 mM EDTA (pH 8.0) (buffer A) and was then homogenized by sonication on ice. Crude lysate was centrifuged at 36,000g for 30 min at 4 °C. After the supernatant fraction was heated at 60 °C for 15 min and cooled in an ice bath for 5 min, it was centrifuged at 36,000g for 30 min at 4 °C. The process was repeated twice, and then the supernatant was fractionated with ammonium sulfate. The precipitate from the salting out at 30% saturated ammonium sulfate was discarded, and the precipitate formed by gradual addition of ammonium sulfate up to 70% saturation was collected by centrifugation at 16,000g for 20 min at 4 °C. After the precipitate was dissolved in buffer A, the solution was dialyzed against the same buffer and was loaded onto a DEAE ion-exchange column equilibrated with buffer A. The column was washed with five volumes of buffer A and eluted out with 20 mM Tris-HCl (pH 8.0), 200 mM NaCl, and 1 mM EDTA. Eluted protein was precipitated by 70% saturated ammonium sulfate and was collected by centrifugation at 16,000g for 20 min. The precipitate was dissolved in buffer A, and then the solution was dialyzed against the same buffer. The solution was loaded onto a MonoQ ion-exchange column (GE Healthcare, Buckinghamshire, UK) equilibrated with buffer A and eluted with a 50 to 500 mM NaCl linear gradient in buffer A. Fractions containing the protein were stored at 4 °C. The resulting enzyme was electrophoretically homogenous, with a specific activity of 2.4 μ mol/min per milligram protein at 60 °C (pH 9.0) in the presence of 1 mM spermidine and purity of 51-fold.⁹ Protein concentrations were estimated with BCA Protein Assay Reagent Kit (Pierce, Rockford, IL) using bovine serum albumin as a standard.

Gel filtration

The molecular mass of the purified protein was determined by gel-filtration analysis. Protein (0.4 mg/ml, 11 μ M as monomer) was passed through a Sephadex 200 HR 10/30 column (GE Healthcare) at a flow rate of 0.2 ml/min in 100 mM Tris–Cl (pH 8.0) and 150 mM NaCl. Ovalbumin (45 kDa, Sigma-Aldrich, St. Louis, MO) and MW-GF-1000 Kit (Sigma-Aldrich) was used for molecular weight markers. The kit contains Blue Dextran (2000 kDa), apoferritin from horse spleen (443 kDa), β -amylase from sweet potato (200 kDa), alcohol dehydrogenase from yeast (150 kDa), and carbonic anhydrase from bovine erythrocytes (29 kDa).

CD measurements

CD spectrum measurements were carried out with a JASCO J-720C (JASCO, Hachioji, Japan) spectropolarimeter. A 0.1-cm cell was used for far-UV CD measurements. The temperature of the sample solution in the cell was controlled with a HAAKE circulating bath (Thermo Fisher Scientific, Inc., Waltham, MA) and programmable temperature controller. The temperature in the cell was monitored with a thermocouple. Scan rate was 1 $^{\circ}$ C/min and protein concentration of the enzyme was 0.2 mg/ml (1.4 μ M as tetramer).

Enzyme assay

The aminopropyltransferase assay was performed as described,³⁸ except as detailed below. Since putrescine was inefficient as a substrate for the enzyme, spermidine was used as a standard substrate instead. The pH of the reaction mixtures was adjusted at the corresponding reaction temperature. [*methyl*-¹⁴C]dcSAM was synthesized according to the method of Samejima and colleagues.³⁹ For measurements of kinetic parameters, the enzymatic reaction was performed in one tube and 100 μ l of reaction mixture was sampled at 0.5, 1, 5, 10, 15, and 20 min. Since dcSAM decomposes spontaneously at high temperature under alkaline conditions,⁴⁰ kinetic parameters were determined at 37 $^{\circ}$ C, pH 9. The K_m for dcSAM was determined by measuring initial velocities of the reaction by changing the concentration (1.2–4.8 μ M) of dcSAM in the presence of a fixed concentration (1 mM) of spermidine with 5 ng of TtTAAPT. K_m values for polyamines were measured by changing the concentration of the polyamine (0.5–2 μ M for spermidine and norspermidine, 10–60 μ M for mitsubishine) in the presence of a fixed concentration (38 μ M) of dcSAM. K_m and k_{cat} of spermidine, norspermidine, and mitsubishine were measured with 10, 10, and 25 ng of TtTAAPT, respectively.

Identification of reaction product

To identify the reaction product of TtTAAPT, 900 μ l of the reaction mixtures consisted of 0.1 M Tris–Cl buffer (pH 9), 5 mM dithiothreitol, 0.36 mM unlabeled dcSAM, and a polyamine (1 mM norspermidine, 2 mM spermidine or agmatine, or 4 mM mitsubishine) as the substrate. The reaction mixtures were incubated with

the purified enzyme (4.5 μ g for norspermidine, 9 μ g for spermidine, agmatine, and mitsubishine) at 37 $^{\circ}$ C for 180 min. The reaction was terminated with 5% perchloric acid and the reaction product was identified by gas chromatography^{26,41} or HPLC.² Gas chromatography was performed with a GC-9A gas chromatograph (Shimadzu, Kyoto, Japan) after heptafluorobutyrylation of the concentrated reaction product. A Pyrex glass column (2.1 m, 3-mm inside diameter) was packed with 3% SE-30. Helium was used as the carrier gas at the flow rate of 40 ml/min. The column oven temperature was programmed from 120 to 280 $^{\circ}$ C at a rate of 15 $^{\circ}$ C/min.

Crystallization, data collection, and processing

The purified protein was dialyzed against 20 mM Tris–HCl and 50 mM NaCl (pH 8.0) and concentrated to approximately 8 mg/ml using a 100-kDa cutoff Centricon (Millipore, Billerica, MA). The initial crystallization trials were carried out using Grid Screen PEG (polyethylene glycol) 6000 and Grid Screen Ammonium Sulfate (Hampton Research, Aliso Viejo, CA) by the hanging-drop vapor-diffusion method (1:1, protein solution to reservoir solution) at 20 $^{\circ}$ C. Crystals were grown in two different conditions: 30% PEG 6000, 0.1 M Tris–HCl (pH 8.0) or 1.6 M ammonium sulfate, 0.1 M 2-(*N*-morpholino)ethanesulfonic acid–NaOH (pH 6.0). Preliminary X-ray work suggested that both crystals belong to the tetragonal space group of either $P4_32_12$ or $P4_32_12$. After optimization of the crystallization conditions, crystals used for structure determination were obtained in 0.1 M 2-(*N*-morpholino)ethanesulfonic acid–NaOH buffer (pH 6.5), containing 1.5 M ammonium sulfate and 3 mM norspermidine at 20 $^{\circ}$ C. The enzyme–SAM complex crystals were obtained under the conditions of 9 mg/ml protein, 1.8 M ammonium sulfate, 0.1 M 2-(*N*-morpholino)ethanesulfonic acid–NaOH buffer (pH 5.5), and 1 mM SAM.

Table 2. Crystallographic data collection and refinement statistics

	Native	SAM complex
<i>Data collection</i>		
Space group	$P4_32_12$	$P4_32_12$
Unit cell (\AA)	$a = 87.78, c = 190.83$	$a = 88.04, c = 191.00$
Resolution (\AA)	40.00–2.00 (2.11–2.00)	20.00–2.50 (2.59–2.50)
No. of reflections		
Observations	561,274	155,196
Unique	49,522	25,838
Completeness	96.7 (85.0)	91.7 (78.3)
Averaged I/σ_I	15.6 (5.1)	11.2 (3.2)
R_{merge} (%)	3.5 (15.9)	11.9 (35.4)
<i>Refinement</i>		
R/R_{free} (%)	19.0/23.8	18.3/26.8
RMSD from ideal ($\text{\AA}, ^{\circ}$)	0.008/1.5	0.030/2.7
Average B -factor ^a	30.7/34.4/37.5/—	38.4/39.3/30.1/56.0
Ramachandran plot ^b	90.2/9.4/0.4/0.0	81.1/17.2/1.3/0.4

Values in parentheses are for the highest-resolution shell.

^a Main chain/side chain/water/ligand.

^b Most favored/additional allowed/generously allowed/disallowed.

Diffraction data were collected with an ADSC Quantum 4R CCD detector at beamline NW12 at the Photon Factory Advanced Ring for the native crystals and an R-Axis detector at a laboratory X-ray source for the binary complex crystals. Crystals were soaked with 20% glycerol as a cryoprotectant and were mounted under a nitrogen stream kept at $-173\text{ }^{\circ}\text{C}$. Data were indexed and scaled with Mosflm and Scala⁴² and CrystalClear/d*TREK programs. Data processing statistics are presented in Table 2.

Structure determination and refinement

The structure was solved by molecular replacement with the program EPMR.⁴³ TmSPDS¹⁷ (PDB ID 1INL) has about 34% identical amino acid sequence with TtTAAPT and was used to construct a model by substitution of all amino acids into serine residues except for alanine and glycine residues. After several cycles of calculations, the best correlation coefficient between observed and calculated structure amplitudes was estimated to be 0.45 with two independent molecules in an asymmetric unit in the space group $P4_32_12$.

The converged molecules were mutated so as to have the same amino acid sequence with TtTAAPT and were refined with the CNS program.⁴⁴ In each cycle of the CNS refinement, each model was rebuilt with the program XtalView/Xfit.⁴⁵ The final model was refined at 2.0 Å resolution to R and free R -factors of 19.9 and 23.9%, respectively. The refined model had geometries with RMSD of 0.008 Å and 1.5° from ideal values for bond lengths and angles, respectively, and was qualified by PROCHECK.⁴⁶ There are two residues (Asp50 of both chains) in the disallowed region; however, they fitted well into the electron density map and are considered to have this conformation actually. The binary complex structure was determined using the native structural model and the inclusion of SAM molecular models as MTA molecules. Refinement statistics are summarized in Table 1.

Structural analyses

The structural modeling for substrate recognition was performed using the binary complex structure in comparison with the 3D structure of TmSPDS-Ado-DATO complex structures.¹⁷ Superimposition of Ado-DATO to SAM was done by least-square minimization of their adenosyl moiety. Instead of the putrescine moiety in Ado-DATO, agmatine and spermidine moieties were constructed using modeling programs MOLDA and Chimera. The model structures were docked into the TtTAAPT structure with the program DOCK version 6.1 with anchor-and-grow mode,⁴⁷ where the adenosyl moieties of the models were treated as the rigid substructure and anchored into the protein model with the least-square result, and the structures of the other polyamine portions were extended as flexible ligands.

Molecular graphics in the figures were drawn with the program PyMOL. Superimposition was carried out with TOP.⁴⁸ Sequence alignments were performed with the program ClustalW⁴⁹ and displayed with ESPript.⁵⁰

Accession numbers

The coordinates and structure factors of the native and binary complex have been deposited in the PDB with accession codes 1UIR and 3ANX, respectively.

Acknowledgements

The authors are grateful to Prof. Seiki Kuramitsu of Osaka University for providing the nucleotide sequence of TtTAAPT. We thank Daisuke Saito for technical assistance, the synchrotron beamline staff at SPring-8, the Photon Factory for crystallographic data collection, Dr. Masaki Yoshida (University of Tsukuba) for phylogenetic analyses, and Dr. Anthony J. Michael (UT Southwestern Medical Center, Dallas, TX) for critical reading of the manuscript. This work was supported in part by Grants-in-Aid for Scientific Research (No. 11794038 and 16657040), for Promoting Bioventures in Private Universities, and for National Project on Protein Structural and Functional Analyses from the Ministry of Education, Culture, Sports, Science and Technology, the Japanese Government.

References

1. Tabor, C. W. & Tabor, H. (1984). Polyamines. *Annu. Rev. Biochem.* **53**, 749–790.
2. Oshima, T. (1983). Novel polyamines in *Thermus thermophilus*: isolation, identification, and chemical synthesis. *Methods Enzymol.* **94**, 401–411.
3. Oshima, T., Hamasaki, N., Senshu, M., Kakinuma, K. & Kuwajima, I. (1987). A new naturally occurring polyamine containing a quaternary ammonium nitrogen. *J. Biol. Chem.* **262**, 11979–11981.
4. Oshima, T., Hamasaki, N. & Uzawa, T. (1988). Biochemical properties of unusual polyamines found in an extreme thermophile, *Thermus thermophilus*. *Adv. Exp. Med. Biol.* **250**, 633–642.
5. Terui, Y., Ohnuma, M., Hiraga, K., Kawashima, E. & Oshima, T. (2005). Stabilization of nucleic acids by unusual polyamines produced by an extreme thermophile, *Thermus thermophilus*. *Biochem. J.* **388**, 427–433.
6. Bell, E. & Malmberg, R. L. (1990). Analysis of a cDNA encoding arginine decarboxylase from oat reveals similarity to the *Escherichia coli* arginine decarboxylase and evidence of protein processing. *Mol. Gen. Genet.* **224**, 431–436.
7. Sekowska, A., Bertin, P. & Danchin, A. (1998). Characterization of polyamine synthesis pathway in *Bacillus subtilis* 168. *Mol. Microbiol.* **29**, 851–858.
8. Pegg, A. E., Shuttleworth, K. & Hibasami, H. (1981). Specificity of mammalian spermidine synthase and spermine synthase. *Biochem. J.* **197**, 315–320.
9. Ohnuma, M., Terui, Y., Tamakoshi, M., Mitome, H., Niitsu, M., Samejima, K. *et al.* (2005). N^1 -Aminopropylagmatine, a new polyamine produced as a key

- intermediate in polyamine biosynthesis of an extreme thermophile, *Thermus thermophilus*. *J. Biol. Chem.* **280**, 30073–30082.
10. Knott, J. M., Römer, P. & Sumper, M. (2007). Putative spermine synthases from *Thalassiosira pseudonana* and *Arabidopsis thaliana* synthesize thermospermine rather than spermine. *FEBS Lett.* **581**, 3081–3086.
 11. Kajander, E. O., Kauppinen, L. I., Pajula, R. L., Karkola, K. & Eloranta, T. O. (1989). Purification and partial characterization of human polyamine synthases. *Biochem. J.* **259**, 879–886.
 12. Wu, H., Min, J., Zeng, H., McCloskey, D. E., Ikeguchi, Y., Loppnau, P. *et al.* (2008). Crystal structure of human spermine synthase: implications of substrate binding and catalytic mechanism. *J. Biol. Chem.* **283**, 16135–16146.
 13. Pegg, A. E. & Michael, A. J. (2010). Spermine synthase. *Cell. Mol. Life. Sci.* **67**, 113–121.
 14. Dufe, V. T., Qiu, W., Müller, I. B., Hui, R., Walter, R. D. & Al-Karadaghi, S. (2007). Crystal structure of *Plasmodium falciparum* spermidine synthase in complex with the substrate decarboxylated S-adenosylmethionine and the potent inhibitors 4MCHA and AdoDATO. *J. Mol. Biol.* **373**, 167–177.
 15. Bowman, W. H., Tabor, C. W. & Tabor, H. (1973). Spermidine biosynthesis. Purification and properties of propylamine transferase from *Escherichia coli*. *J. Biol. Chem.* **248**, 2480–2485.
 16. Zhou, X., Chua, T. K., Tkaczuk, K. L., Bujnicki, J. M. & Sivaraman, J. (2010). The crystal structure of *Escherichia coli* spermidine synthase SpeE reveals a unique substrate-binding pocket. *J. Struct. Biol.* **169**, 277–285.
 17. Korolev, S., Ikeguchi, Y., Skarina, T., Beasley, S., Arrowsmith, C., Edwards, A. *et al.* (2002). The crystal structure of spermidine synthase with a multisubstrate adduct inhibitor. *Nat. Struct. Biol.* **9**, 27–31.
 18. Dams, T., Auerbach, G., Bader, G., Jacob, U., Ploom, T., Huber, R. & Jaenicke, R. (2000). The crystal structure of dihydrofolate reductase from *Thermotoga maritima*: molecular features of thermostability. *J. Mol. Biol.* **297**, 659–672.
 19. Maeda, N., Kanai, T., Atomi, H. & Imanaka, T. (2002). The unique pentagonal structure of an archaeal Rubisco is essential for its high thermostability. *J. Biol. Chem.* **277**, 31656–31662.
 20. Salminen, T., Teplyakov, A., Kankare, J., Cooperman, B. S., Lahti, R. & Goldman, A. (1996). An unusual route to thermostability disclosed by the comparison of *Thermus thermophilus* and *Escherichia coli* inorganic pyrophosphatases. *Protein Sci.* **5**, 1014–1025.
 21. Vieille, C. & Zeikus, G. J. (2001). Hyperthermophilic enzymes: sources, uses, and molecular mechanisms for thermostability. *Microbiol. Mol. Biol. Rev.* **65**, 1–43.
 22. Bagga, S., Rochford, J., Klaene, Z., Kuehn, G. D. & Phillips, G. C. (1997). Putrescine aminopropyltransferase is responsible for biosynthesis of spermidine, spermine, and multiple uncommon polyamines in osmotic stress-tolerant alfalfa. *Plant Physiol.* **114**, 445–454.
 23. Wu, H., Min, J., Ikeguchi, Y., Zeng, H., Dong, A., Loppnau, P. *et al.* (2007). Structure and mechanism of spermidine synthases. *Biochemistry*, **46**, 8331–8339.
 24. Cacciapuoti, G., Porcelli, M., Moretti, M. A., Sorrentino, F., Concilio, L., Zappia, V. *et al.* (2007). The first agmatine/cadaverine aminopropyl transferase: biochemical and structural characterization of an enzyme involved in polyamine biosynthesis in the hyperthermophilic archaeon *Pyrococcus furiosus*. *J. Bacteriol.* **189**, 6057–6067.
 25. Oshima, T. (1989). Polyamines in thermophiles. In *The Physiology of Polyamines* (Bachrach, J. & Heimer, Y. M., eds), vol. 2, pp. 36–46. CRC Press, Inc., Boca Raton, FL.
 26. Niitsu, M., Samejima, K., Matsuzaki, S. & Hamana, K. (1993). Systematic analysis of naturally occurring linear and branched polyamines by gas chromatography and gas chromatography–mass spectrometry. *J. Chromatogr.* **641**, 115–123.
 27. Kagawa, Y., Nojima, H., Nukiwa, N., Ishizuka, M., Nakajima, T., Yasuhara, T. *et al.* (1984). High guanine plus cytosine content in the third letter of codons of an extreme thermophile. DNA sequence of the isopropylmalate dehydrogenase of *Thermus thermophilus*. *J. Biol. Chem.* **259**, 2956–2960.
 28. Jaenicke, R. & Bohm, G. (1998). The stability of proteins in extreme environments. *Curr. Opin. Struct. Biol.* **8**, 738–748.
 29. Hanzawa, Y., Takahashi, T., Michael, A. J., Burtin, D., Long, D., Pineiro, M. *et al.* (2000). *ACAULIS5*, an *Arabidopsis* gene required for stem elongation, encodes a spermine synthase. *EMBO J.* **19**, 4248–4256.
 30. Hashimoto, T., Tamaki, K., Suzuki, K. & Yamada, Y. (1998). Molecular cloning of plant spermidine synthases. *Plant Cell Physiol.* **39**, 73–79.
 31. Hanzawa, Y., Imai, A., Michael, A. J., Komeda, Y. & Takahashi, T. (2002). Characterization of the spermidine synthase-related gene family in *Arabidopsis thaliana*. *FEBS Lett.* **527**, 176–180.
 32. Imai, R., Ali, A., Pramanik, H. R., Nakaminami, K., Sentoku, N. & Kato, H. (2004). A distinctive class of spermidine synthase is involved in chilling response in rice. *J. Plant Physiol.* **161**, 883–886.
 33. Tabor, C. W. & Tabor, H. (1987). The *speEspeD* operon of *Escherichia coli*. Formation and processing of a proenzyme form of S-adenosylmethionine decarboxylase. *J. Biol. Chem.* **262**, 16037–16040.
 34. Orr, G. R., Danz, D. W., Pontoni, G., Prabhakaran, P. C., Gould, S. J. & Coward, J. K. (1988). Synthesis of chirally deuterated (S-adenosyl-S-methylsulfonyl)propylamines and spermidines. Elucidation of the stereochemical course of putrescine aminopropyltransferase (spermidine synthase). *J. Am. Chem. Soc.* **110**, 5791–5799.
 35. Dufe, V. T., Luersen, K., Eschbach, M. L., Haider, N., Karlberg, T., Walter, R. D. *et al.* (2005). Cloning, expression, characterisation and three-dimensional structure determination of *Caenorhabditis elegans* spermidine synthase. *FEBS Lett.* **579**, 6037–6043.
 36. Yamamoto, S., Nagata, S. & Kusaba, K. (1993). Purification and characterization of homospermidine synthase in *Acinetobacter tartarogenes* ATCC 31105. *J. Biol. Chem.* **114**, 45–49.
 37. Stamatakis, A., Hoover, P. & Rougemont, J. (2008). A rapid bootstrap algorithm for the RAxML Web servers. *Syst. Biol.* **57**, 758–771.
 38. Raina, A., Eloranta, T. & Pajula, R. (1983). Rapid assays for putrescine aminopropyltransferase (spermidine synthase) and spermidine aminopropyltransferase (spermine synthase). *Methods Enzymol.* **94**, 257–260.

39. Dejima, H., Kobayashi, M., Takasaki, H., Takeda, N., Shirahata, A. & Samejima, K. (2003). Synthetic decarboxylated S-adenosyl-L-methionine as a substrate for aminopropyl transferases. *Biol. Pharm. Bull.* **26**, 1005–1008.
40. Zappia, V., Galletti, P., Oliva, A. & de Santis, A. (1977). New methods for preparation and analysis of S-adenosyl-(5')-3-methylthiopropylamine. *Anal. Biochem.* **79**, 535–543.
41. Hamana, K., Niitsu, M., Samejima, K., Itoh, T., Hamana, H. & Shinozawa, T. (1998). Polyamines of thermophilic eubacteria belonging to the genera *Thermotoga*, *Thermodesulfovibrio*, *Thermoleophilum*, *Thermus*, *Rhodothermus* and *Meiothermus*, and the thermophilic archaeobacteria belonging to the genera *Aeropyrum*, *Picrophilus*, *Methanobacterium* and *Methanococcus*. *Microbios*, **94**, 7–21.
42. Collaborative Computational Project, Number 4 (1994). The CCP4 suite: programs for protein crystallography. *Acta Crystallogr., Sect. D: Biol. Crystallogr.* **50**, 760–763.
43. Kissinger, C. R., Gehlhaar, D. K. & Fogel, D. B. (1999). Rapid automated molecular replacement by evolutionary search. *Acta Crystallogr., Sect. D: Biol. Crystallogr.* **55**, 484–491.
44. Brünger, A. T., Adams, P. D., Clore, G. M., DeLano, W. L., Gros, P., Grosse-Kunstleve, R. W. *et al.* (1998). Crystallography & NMR system: a new software suite for macromolecular structure determination. *Acta Crystallogr., Sect. D: Biol. Crystallogr.* **54**, 905–921.
45. McRee, D. E. (1999). XtalView/Xfit—a versatile program for manipulating atomic coordinates and electron density. *J. Struct. Biol.* **125**, 156–165.
46. Laskowski, R. A., MacArthur, M. W., Moss, D. S. & Thornton, J. M. (1993). PROCHECK—a program to check the stereochemical quality of protein structures. *J. Appl. Crystallogr.* **26**, 283–291.
47. Brooijmans, N. & Kuntz, I. (2003). Molecular recognition and docking algorithms. *Annu. Rev. Biophys. Biomol. Struct.* **32**, 335–373.
48. Lu, G. (2000). TOP: a new method for protein structure comparisons and similarity searches. *J. Appl. Crystallogr.* **33**, 176–183.
49. Thompson, J. D., Higgins, D. G. & Gibson, T. J. (1994). CLUSTAL W: improving the sensitivity of progressive multiple sequence alignment through sequence weighting, position-specific gap penalties and weight matrix choice. *Nucleic Acids Res.* **22**, 4673–4680.
50. Gouet, P., Courcelle, E., Stuart, D. I. & Metz, F. (1999). ESPript: analysis of multiple sequence alignments in PostScript. *Bioinformatics*, **15**, 305–308.